Received: 21 August 2018 | Revised: 21 May 2019 | Accepted: 29 May 2019 | Published on: 28 June 2019

DOI: 10.1002/joc.6182

RESEARCH ARTICLE

International Journal of Climatology RMetS

Change in the spatiotemporal pattern of snowfall during the cold season under climate change in a snow-dominated region of China

Lei Bai[1,2,3] | **Chunxiang Shi**[4] | **Qingdong Shi**[1] | **Lanhai Li**[3] | **Jing Wu**[5] | **Yanfen Yang**[6] | **Shuai Sun**[4] | **Feiyun Zhang**[7] | **Junyao Meng**[8]

[1]State Key Laboratory of Desert and Oasis Ecology, Xinjiang Institute of Ecology and Geography, Chinese Academy of Sciences, Urumqi, China

[2]University of Chinese Academy of Sciences, Beijing, China

[3]College of Resources and Environmental Science, Xinjiang University, Urumqi, China

[4]National Meteorological Information Center, Beijing, China

[5]Lanzhou Central Meteorological Observatory, Lanzhou, China

[6]State Key Laboratory of Soil Erosion and Dryland Farming on the Loess Plateau, Institute of Soil and Water Conservation, Northwest A&F University, Yangling, China

[7]Faculty of Management, Xinjiang Agricultural University, Urumqi, China

[8]Chiyuan Science Technology, Beijing, China

Correspondence
Chunxiang Shi, National Meteorological Information Center, 100081 Beijing, China.
Email: shicx@cma.gov.cn

Funding information
Key Program of National Natural Science Foundation of China, Grant/Award Number: 91437220, 41501301; Science & Technology Basic Resources Investigation Program of China, Grant/Award Number: 2017FY100501_5; the R& D Special Fund for Public Welfare Industry (Meteorology), Grant/Award Number: GYHY201506002

Abstract

The spatiotemporal pattern of precipitation is significantly changing with global climate change. Snowfall is a solid phase of precipitation and an important water resource. With two gridded data sets of APHRO (Asia Precipitation-Highly-Resolved Observational Data Integration Towards Evaluation of Water Resources) and CN05.1, this study analyses the changes in the spatiotemporal pattern of snowfall in a snow-dominant region of China from 1961 to 2015. The results indicate the significant increasing trend of winter snowfall in horizontal and altitude dimension in snow-dominant regions, but the winter snowing season length shortened. For the frequency of snowfall intensity level, light, and heavy snowfall and snowstorms increased, but moderate snowfall showed no change. However, the intensity of extreme snowfall in once-in-a-century was decreasing in all of the snow-dominant regions. In the altitude dimension, the increasing trend in snow-dominant conditions was not uniform, which may be related to change in air temperature and water vapour through the vertical atmospheric levels. The upwards trend in snowfall may be caused by the increase of atmospheric water content rather than the change of snowy weather conditions. In addition, the change values of climate indices can also contribute to snowfall increasing in snow-dominant regions.

KEYWORDS

northeast China, precipitation phase, Qinghai-Tibet Plateau, warming, Xinjiang

1 | INTRODUCTION

Snowfall is one of the solid phases of precipitation that affects the ecological environment and hydrological processes in mountainous areas (Barnett *et al*., 2005; Jonas *et al*., 2008) and water resource management (Duethmann *et al*., 2014; Mankin *et al*., 2015). Furthermore, snowfall supplies the glacier, streams, and groundwater (Zhang *et al*., 2014; Zhang *et al*., 2016b) and impacts surface energy balance processes, heat and water transportation in soil (Fu *et al*., 2018), spatiotemporal patterns of vegetation (Chen *et al*., 2015; Li *et al*., 2015), and climate evolution in the following warm season (Davis *et al*., 2005; Dash *et al*., 2006).

Under climate change, studies focused on spatiotemporal pattern of snowfall in China began with in situ observations. After 1980, the precipitation phase is not labelled (Ding *et al*., 2014). The long-term spatiotemporal pattern of snowfall is studied using snowfall data series after partitioning the precipitation phase (Liu *et al*., 2012b; Sun *et al*., 2012; Zhang *et al*., 2016a). However, the surface meteorological observation network is relatively evenly distributed in eastern China and sparsely distributed in western China. Moreover, snowfall occurs more frequently in western China than in eastern China (e.g., the Qinghai-Tibet Plateau). Thus, the analysis of the spatiotemporal pattern of snowfall with in situ observations has great spatial uncertainty in western China. Following the development of retrieval algorithms for snowfall–emission reflection (Fujiyoshi *et al*., 1990; Borys *et al*., 2003), Doppler Weather Radar (DWR) had provided a snowfall product with high temporal and spatial resolution. However, although there are 199 DWRs in China, which are evenly distributed as surface meteorological observation network in eastern China, the provision of data for western China remains limited. In China, there is no snow data assimilation system with a clear mechanism like the U.S. Snow Data Assimilation System (SNOWDAS; National Operational Hydrologic Remote Sensing Center, 2004). Thus, a high spatiotemporal resolution snowfall product is not yet available for related research. However, the gridded precipitation (including rainfall and snowfall) extrapolated by rational hypothesis is a potential gridded observation with less uncertainty and more rational spatial pattern than that obtained directly from in situ observation (Shen and Xiong, 2016).

Numerical weather models contain a cloud microphysics scheme, which describes the water vapour exchange process between cloud water and cloud ice. Thus, global climate models (GCMs), the numerical weather prediction (NWP) model, and reanalysis data sets with the atmospheric data assimilation technique can directly output the snowfall variable. Therefore, the long-term gridded snowfall is typically taken from coarse grid reanalysis data sets, such as ERA40 (Uppala *et al*., 2005), JRA55 (Kobayashi *et al*., 2015), NCEP/NCAR (Kalnay *et al*., 1996), NOAA-CIRES (Compo *et al*., 2006), and ERA20C (Poli *et al*., 2016), for which temporal coverage is more than half a century. However, these reanalysis data sets have coarse resolution and thus cannot describe the micro-atmospheric processes caused by the complex terrain in snow-dominated regions of western China. Although there are several regional atmospheric data assimilation data sets with high spatiotemporal resolution (Maussion *et al*., 2014; Ma *et al*., 2016), the snowfall has different spatiotemporal patterns even in the same simulation region, which is affected by atmospheric forcing and cloud microphysics process. This increases the uncertainty of estimations of snowfall spatiotemporal evolution. The Global Precipitation Measurement (GPM) Mission, which is the subsequent mission of Tropical Rainfall Measuring Mission (TRMM), was launched in 2014 and has the ability to detect the snowfall with dual-frequency precipitation radar (Hou *et al*., 2014). However, snowfall from GPM precipitation data set has higher spatial and temporal resolution than reanalysis data sets, and the snowfall retrieval algorithm depends on empirical and statistical equation and humidity from reanalysis data sets. Therefore, the GPM snowfall product needs more evaluation in China before it can be used in application.

Previous studies related to snowfall in China are mainly concerned with the climatological trend, the ratio between snowfall and rainfall (Laternser and Schneebeli, 2003), and the change of its spatiotemporal pattern (Li *et al*., 2012; Sun *et al*., 2012; Liu *et al*., 2012b; Zhu *et al*., 2014; Jiang *et al*., 2016; Zhang *et al*., 2016a). They do not provide a hypothesis for changes in spatiotemporal pattern of snowfall change under climate change. Furthermore, these studies' areas are mainly focused on western China (e.g., Xinjiang and the Qinghai-Tibet Plateau), and few studies systematically study the entire snowcover-dominated regions in China. It has been shown that snowfall has a significant change on spatial patterns in alpine regions and plains (Laternser and Schneebeli, 2003; Marty, 2008; Yamaguchi *et al*., 2011). The studies focused on the Qinghai-Tibet Plateau (Wang *et al*., 2016a; Deng *et al*., 2017) also lack the examination of altitude dimension.

In this study, we focused on analysing the changes in spatiotemporal pattern of snowfall in both horizontal and altitude dimensions with gridded snowfall data sets, and identifying possible reasons accounting for the changes in snowfall under over 50 years. The remaining parts of this paper are organized as follows: section 2 introduces the data sets and the methods. Section 3 contains the analysis of changes in snowfall spatiotemporal distribution and intensity, and analysis of possible reasons for these changes. Section 4 discusses the results and section 5 provides the key conclusions of this research.

2 | METHODOLOGY AND DATA SETS

2.1 | Study area

China has three stable periodically snow-dominated regions, northern Xinjiang (XN), northeast China (NE), the Qinghai-Tibet Plateau (TP; Sun *et al*., 2010a; Liu *et al*., 2012c). The elevation range of these three regions on the grid of 0.25° (Figure 1) is 310–3,830 m, 50–1,180 m, and 2,700–5,500 m, respectively.

The transitional views consider the sub-alpine region between 1,000 and 3,500 m a.s.l., and plain regions between 500 and 1,000 m a.s.l. Thus, no sub-alpine and plain regions in Qinghai-Tibet Plateau. To avoid this problem, the percentile method was applied to discretize the elevation range into three zones in the snow-dominant region. This approach uses the lower and upper percentile of areas of 33.3 and 66.6% of the total area, respectively. This approach was taken rather than the clustering method because the clustering method would lead to areas with few in situ sample points and thus some zones with less representation. The elevation (DEM) data comes from the GTOP30 DEM dataset (http://www1.gsi.go.jp/geowww/globalmap-gsi/gtopo30/gtopo30.html), which horizontal resolution of 1 km and is resampled into a 0.25° grid. A detailed description of elevation zones is shown in Table 1.

2.2 | Data sets

In this study, several gridded data sets (Table 2) were employed for generation of the gridded snowfall data, comparison of the significance of snowfall change at multiple scales, and the analysis for possible reasons accounting for snowfall change. These data sets are described in detail in this section.

2.2.1 | Gridded in situ observations

The CN05.1 data set, generated and maintained by the National Climate Center, Chinese Meteorological Administration, was extrapolated by the thin plate spline method using more than 2,400 in situ stations across China for 1961–2015 (Wu and Gao, 2013). Furthermore, these data sets have already been used in TP (Wang *et al*., 2018). In this study, daily mean temperature, daily relative humidity, and daily precipitation were used. The Asia Precipitation-Highly-Resolved Observational Data Integration Towards Evaluation of Water Resources (APHRO) dataset covers the whole of East Asia and has temporal coverage of 1961–2007 (Yatagai *et al*., 2012), including the variables of daily mean temperature and daily total precipitation. Furthermore, a flag is provided for the precipitation phase in APHRO to assist in the separation of precipitation into snowfall. In general, the number

TABLE 1 Description of the boundaries of elevation zones in snow-dominant regions (units: m)

Regions	Zone 1 (Z1)	Zone 2 (Z2)	Zone 3 (Z3)
Qinghai-Tibet Plateau (TP)	2,700–4,180	4,180–4,840	4,840–5,550
Northeast China (NE)	50–400	400–650	650–1,180
Northern Xinjiang (XN)	310–1,060	1,060–1,780	1,780–3,830

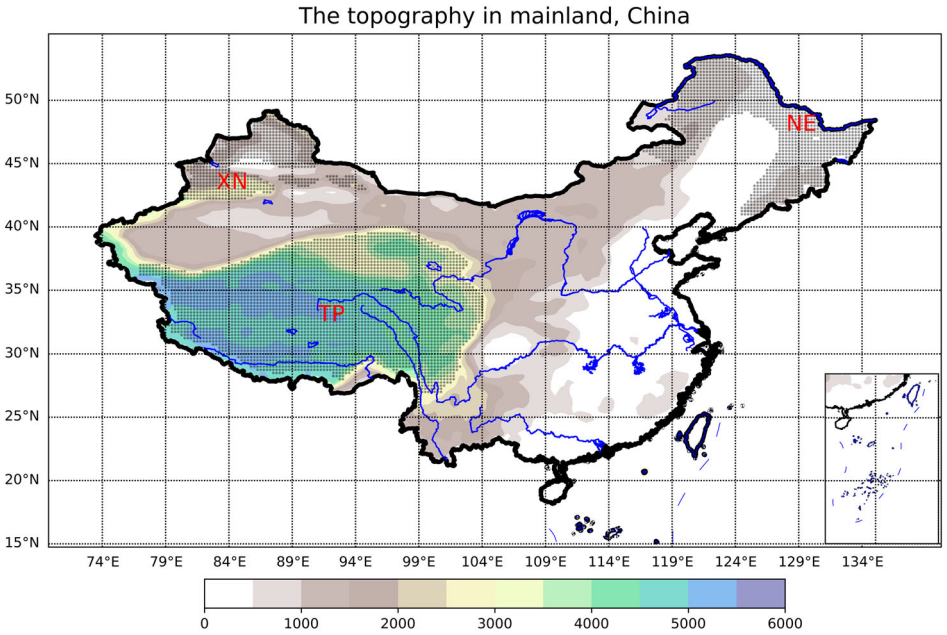

FIGURE 1 The topography of mainland China and subregions. The rivers are drawn in blue lines. The shaded regions are snow-dominated regions. XN, TP, and NE indicate for northern Xinjiang, the Qinghai-Tibet Plateau, and northeast China, respectively [Colour figure can be viewed at wileyonlinelibrary.com]

TABLE 2 The datasets used in this study

Data sets	Temporal coverage/resolution	Spatial resolution	Variable	Usage
1. CN05.1	1961–2016/daily	0.25°	Temperature, precipitation	Making gridded snowfall data sets
2. APHRO	1961–2007/daily	0.25°	Temperature, precipitation	Making gridded snowfall data sets
3. CRU	1901–2012/monthly	0.5°	Precipitation	Long-term trend analysis
4. WM	1901–2015/monthly	0.5°	Precipitation	Long-term trend analysis
5. GPCC	1901–2015/monthly	0.5°	Precipitation	Long-term trend analysis
7. NCEP/NCAR reanalysis data set	1948–2017/6 hr	2.5°	Temperature, *U* and *V* wind, specific humidity, geopotential height	Analysis for cause of snowfall change in snow-dominant regions

of in situ stations used in APHRO for China is approximately 800 less than CN05.1. This may reduce the accuracy of APHRO-based snowfall data relative to that of CN05.1. However, both data sets have high horizontal resolution of 0.25°. In addition to APHRO and CN05.1, this study employs well-known long-term climatic datasets including CRU (The Climatic Research Unit) (Harris *et al*., 2014), WM (global [land] precipitation and temperature: Willmott & Matsuura, University of Delaware) (Willmott and Matsuura, 2001), and GPCC (GPCC Global Precipitation Climatology Centre monthly precipitation dataset) (Rudolf *et al*., 1994) to compare the trend of winter precipitation/snowfall in the Northern Hemisphere and China for centennial periods.

2.2.2 | Other gridded data sets

The NCEP/NCAR reanalysis data set (Kalnay *et al*., 1996), which has temporal interval of 6 hr in 1948–2017 with a spatial grid of 2.5°, is used in analysis of snowfall change from thermodynamic process. The air temperature, specific humidity (*Q*), geopotential height, U wind, and V wind were selected at standard isobaric level of 1,000, 925, 850, 700, 600, and 500 hPa. In addition, the partial correlation analysis was calculated with the R software package with bootstrap method.

2.2.3 | Climate indices

Except for mesoscale weather systems (Front, Cyclone, Tough, etc.), which can induce and affect the snowfall process, large-scale weather systems can also affect the snowfall's spatiotemporal pattern (Seager *et al*., 2010). Thus, in this study four climate indices are collected, namely the North Atlantic Oscillation Index (NAO) in 1950–2018 (CPC—Monitoring and Data: Daily North Atlantic Oscillation Index 2004), Arctic Oscillation Index (AO) in 1950–2018 (CPC—Teleconnections: Arctic Oscillation, https://www.cpc.ncep.noaa.gov/products/precip/CWlink/daily_ao_index/ao.shtml [accessed 8th March 2019]), Antarctic Oscillations Index (AAO) in 1979–2018 (CPC—Teleconnections: Antarctic Oscillation, https://www.cpc.ncep.noaa.gov/products/precip/CWlink/daily_ao_index/aao/aao.shtml [accessed 8th March 2019]), and Multivariate ENSO Index (MEI) in 1950–2018 (Team, https://www.esrl.noaa.gov/psd/enso/mei/index.html [accessed 8th March 2019]). To analysis the teleconnection relationship between climate indices and snowfall in China (including the snow-dominated regions), Pearson correlation coefficient is used to calculate climate indices and snowfall in cold season in 1961–2015.

2.3 | The method for partition of precipitation phase

Precipitation has two main phases: solid precipitation (e.g., snowfall) and liquid precipitation (e.g., rainfall). At present, most rain gauges in China do not have the ability to measure solid precipitation. However, the related scientific research fields concerning precipitation usually require partitioning of the precipitation into solid phase and liquid phase because the precipitation in solid phase does not contribute immediately to runoff and is stored as snow cover until the air temperature becomes high enough to melt it into liquid water. In this study, snow sublimation was ignored. Thus, for snow science models and hydrological models within a land surface model, the parameter to partition precipitation is a key optimization goal. With respect to previous studies, two typical methods were applied for this study. The first method, atmospheric temperature profile analysis (Rauber *et al*., 2001; Thériault *et al*., 2006), considers the precipitation as snowfall when the air temperature is below 0°C at a specified isothermal height. The second method is the temperature threshold method (Yang *et al*., 1997; Chen *et al*., 2014; Ding *et al*., 2014), which involves distinguishing precipitation based on the surface air temperature or surface wet bulb temperature threshold. When surface temperature decreases under the temperature threshold, the precipitation is distinguished as snowfall.

In this study, two temperature threshold methods were used (presented in section 3.5). In other sections, however, the only one temperature threshold called temperature–relative–humidity threshold method was used. Here, tm and rh-tm represent the single temperature threshold method (Equation (1)) (Yang *et al*., 1997) and temperature–relative–humidity threshold method (Equation (2)) (Yasutomi *et al*., 2011), respectively. The detailed description of snowfall detecting algorithm is as follows:

$$P_{\text{snowfall}} = \begin{cases} P, T \le T_{\text{threshold}} \\ 0, T > T_{\text{threshold}} \end{cases}, \quad (1)$$

where T is the daily mean air temperature at 2 m height of the ground surface, $T_{\text{threshold}}$ is the threshold for partitioning the rainfall and snowfall in single temperature threshold method. Normally, $T_{\text{threshold}}$ is set from −1 to 4°C by experience. In this study, the calculation is based on a grid scale, not in situ. According to a previous study on grid scale (Yang *et al*., 1997), $T_{\text{threshold}}$ is 2°C,

$$\text{RH}_{\text{cri}} = 92.5 - 7.5T, \quad (2)$$

where RH_{cri} is the daily mean relative humidity threshold for partitioning the rainfall and snowfall in temperature–relative–humidity threshold method. When the daily relative humidity is greater than RH_{cri}, the current precipitation phase is considered as snowfall.

2.4 | The definition of the hydrological period

With reference to the temporal coverage of XN, NE, and TP in a year, the winter time (the cold season) was defined from previous November–March. When calculating the amount of annual snowfall, this study used the hydrological year (September 1 to August 31) as statistical window in sections 3.1 and 3.2. The snowfall statistics and snowy season length calculation were based on hydrological year. The first and final days of snow were the date of first snowfall occurring and the date of the last snowfall, respectively. Julian date was used for convenience of calculation in section 3.4.

2.5 | The snowfall intensity

According to previous studies (Liu *et al*., 2012c) the snowfall was divided into four intensity bins. In the statistical temporal 24-hr windows, the snowfall intensity was classified as light snowfall (<2.5 mm/day), moderate snowfall (2.5–4.9 mm/day), heavy snowfall (5.0–9.9 mm/day), and snowstorm (>10 mm/day).

2.6 | The return period of extreme snowfall

The Gumbel distribution is an Extreme I type distribution. This distribution can reflect the extreme probability characteristics of some meteorological variables (Matti *et al*., 2016). The probability distribution function is shown in (Equation (3)).The extreme snowfall calculation using the Gumbel distribution was conducted according to (Equations (3)–(8)),

$$F(x) = \exp\{-\exp[-\alpha(x-\beta)]\}, \quad (3)$$

where $\alpha > 0$ is the scale parameter, β is the location parameter, and x is the snowfall.

In the parameter estimation, this study used the *L*-moment estimation method, which is a linear combination of probability weight moments. The sample data were sorted in descending order. Finally, an unbiased estimate was obtained for each order,

$$b_r = \frac{1}{n}\sum_{j=1}^{n-r}\frac{C_{n-j}^{r}}{C_{n-1}^{r}}x_j. \quad (4)$$

Next, Equation (4) is linearly combined to obtain the *L*-moment estimate,

$$\hat{\mu}_1 = b_0, \quad (5)$$

$$\hat{\mu}_2 = 2b_1 - b_0. \quad (6)$$

Therefore, Gumbel distribution parameters can be obtained from formula below:

$$\hat{\alpha} = \ln\frac{2}{\mu_2}, \quad (7)$$

$$\beta = \mu_1 - \frac{c}{\hat{\alpha}}, \quad (8)$$

where $c = 0.57722$ is the Euler constant, $\hat{\alpha}$ is the estimated value of the scale parameter, and $\hat{\beta}$ is the estimated value of the location parameter. For smoothing, an 11-year time window was adopted for calculation of winter extreme snowfall intensity in once-in-a-century.

3 | RESULTS

3.1 | Spatial pattern and trend of snowfall

Through the period 1961–2007, the climatological spatial pattern of winter snowfall in APHRO and CN05.1 has mainly remained the same, but with different snowfall intensity. In XN and the mountainous regions on the TP, the

CN05.1 (Figure 2b) showed more snowfall than APRHO (Figure 2a). In XN and NE, the winter snowfall in mountainous regions was greater than that in basin or low-elevation zones. In the TP, the eastern part and Himalayan Mountains had more snowfall than the interior regions. Moreover, in the snow-dominant regions, there was a snowfall of approximately 50 mm in mountainous regions (e.g., Taihang Mountains [113.6°E, 37.4°N] and Qingling Mountains [108.6°E, 33.65°N]).

The tendency of snowfall in most of mainland China is upwards (Figure 2c,d), which is confirmed by in situ observation (Sun *et al*., 2010a; Xu, 2011; Songzhu *et al*., 2014); in particular, northeastern and northwestern China exhibit a strikingly positive linear trend (Sun *et al*., 2012). A significant increasing linear trend in XN was found in both of the snowfall datasets. In Xinjiang, the snowfall shows an increasing trend in 1961–2013 with sparse in situ observation (Wang *et al*., 2017). Moreover, the snow depth had increased, especially in the Tianshan Mountains (84°E, 43°N) (Liequn *et al*., 2013). As snow depth is an indicator of snowfall's change, it indirectly illustrates that snowfall has increased.

However, the patterns in TP and NE were not consistent. In CN05.1 (Figure 2d), the snowfall shows a strikingly increasing trend (>5 mm/10 years) in eastern part of NE, which contrasted with a slightly increasing trend (<2.5 mm/10 years) shown by APRHO (Figure 2c). The previous study with observation in situ shows that mountainous regions in NE including the Great Khingan Mountains (122°E, 47°N) and Lesser Khingan Mountains (125°E, 47°N) had an upwards trend of snowfall in 1960–2005 (Sun *et al*., 2010b). This is well consistent with the grid analysis result in this study. The previous study also points out that the snowfall in the Changbai Mountains (125°E, 40°N) has declined (Sun *et al*., 2010b). Snowfall in APRHO (Figure 2c) shows a declining trend, but CN05.1 shows a strong increasing trend.

The APHRO data set (Figure 2c) indicated a declining trend in western TP and rising trend in the eastern TP. However, the CN05.1 dataset (Figure 2d) revealed a slight declining trend in the TP. One study based on a grid of 0.5° also shows the downwards tendency of snowfall (Wang *et al*., 2016b). Meanwhile, a study with gauge observations, reanalyses, and satellite retrievals increasing trends in spring and winter, which also uses the APHRO precipitation dataset (Tong *et al*., 2014). Even in eastern TP, the snow line of the Qilian Mountains retrieved by the satellite snow product of MODIS has been declining, which reveals that winter snowfall in the cold season has increased (Wang, 2008). Additionally, there are some regional

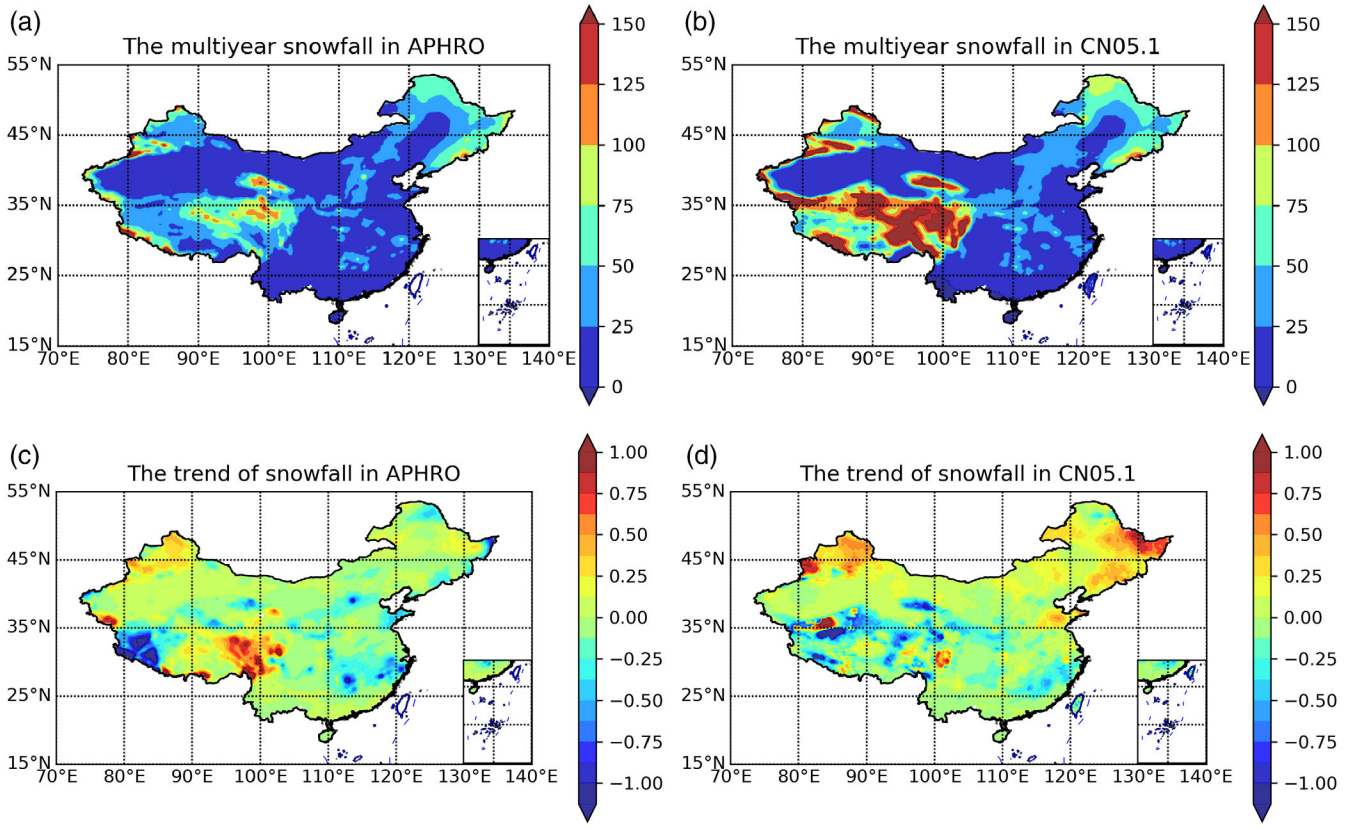

FIGURE 2 Multiyear mean spatial distribution of snowfall (mm/year) in APHRO (a) and CN05.1 (b), and the trend of winter snowfall (mm/year) in APHRO (c) and CN05.1 (d)

studies showing that snowfall tends significantly increase mostly in the TP area (Ke *et al*., 2009; Deng *et al*., 2017). Therefore, the winter snowfall trend showed great uncertainty in TP and NE, which comes from the origin of the APHRO and CN05.1 datasets.

3.2 | Trend of snowfall amount

The decadal change of winter snowfall in snow-dominant regions of China is associated with global winter precipitation change under global climate change. We should therefore compare the winter precipitation or snowfall trend in the boreal hemisphere (NH), China, and snow-dominant regions to reveal the possible linkage to these changes. Based on CRU, WM, and GPCC (Figure 3a), it was found that the winter precipitation anomaly in the NH changed in a small fluctuation in 1901–2012. After 1950, the winter precipitation anomaly increase in China agreed with the change in the NH. Nevertheless, the winter precipitation anomaly in China remained in positive phase, except for a short period in 1961–1980 compared to the reference period of 1961–1990. In the NH, the uncertainty of winter precipitation anomaly was larger than that in China. After the 1960s, the winter precipitation anomaly uncertainty in China decreased, which CRU, WM, and GPCC's ensemble means could reveal a similar trend in the winter precipitation anomaly.

In the 1980s and 1990s, the winter precipitation anomaly in China reached the peak and subsequently decreased. Previous study shows snowfall has significantly increased in snow-dominated regions of China (Sun *et al*., 2010a; Zhang *et al*., 2016a). This illustrates that the winter snowfall contributes to the increase of the winter precipitation in China. In Figure 3b, the analysis with grid data sets in this study also shows that the snowfall in snow-dominant regions exhibits a strong rising trend without complex fluctuation. From mid-1960 to mid-1970, NE's snowfall was in a shortage state. In subsequent times, snowfall began to increase (Li *et al*., 2008; Zhao *et al*., 2009; Sun *et al*., 2010a; 2010b). For XN, snowfall showed an increasing trend in the last 50 years (Peiji, 2001). Thus, the anomaly in NE and XN, which show a significant upwards tendency, agrees with the temporal pattern in previous studies. In TP, anomalies in the late-1970s, late-1980s, late-1990s, and mid-2000s are in a positive phase, which is in agreement with in situ observation studies (Jiang *et al*., 2016).

The altitude distribution of snowfall in snow-dominant regions could indicate the change of atmospheric temperature and water vapour in the vertical dimension. In general, the snowfall in snow-dominant regions displayed a rising trend in all altitude zones. In the TP, the anomaly switched into positive phase from negative phase in 1972–1973, and the anomaly in Zone 1 and Zone 2 was higher than that in Zone 3 (Figure 4a). The same phenomenon occurred in NE (Figure 4b) and XN (Figure 4c). It was thus assumed that the snowfall is increasing at some specific altitude, rather than uniformly increasing in all altitude zones. This may be caused by the water vapour and change in the air temperature on vertical atmospheric levels. Previous study has indicated that the high-altitude zone in the TP is experiencing a warming process (Norris *et al*., 2015), which could result in water vapour change according to Clausius equation. This could cause the water vapour redistribution at both the spatial and temporal scale in the TP and consequently, redistribution of the snowfall.

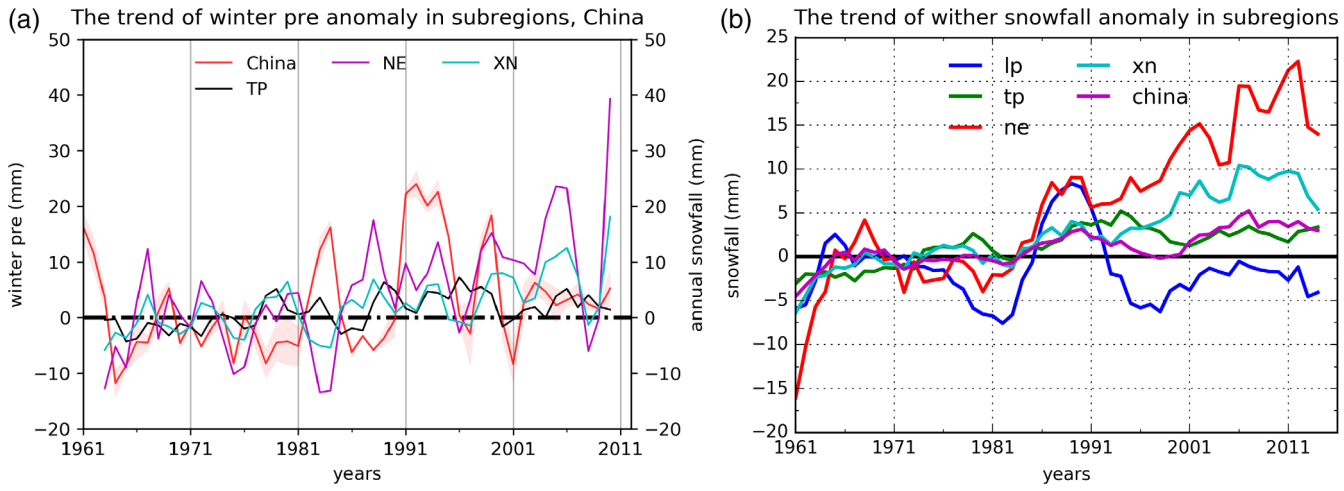

FIGURE 3 The trend of the winter precipitation anomaly in the Northern Hemisphere and China. The blue and the red lines indicate the winter precipitation anomaly averaged over the Northern Hemisphere and China, respectively. The anomaly's reference period is 1961–1990 and the analysis period is 1901–2012. TP, NE, and XN represent Qinghai-Tibet Plateau, northeast China, and northern Xinjiang, respectively. The snowfall anomaly is calculated from the snowfall data set derived from CN05.1. The line is smoothed by a 3-point filter. The shadow area indicates the anomaly's standard deviation [Colour figure can be viewed at wileyonlinelibrary.com]

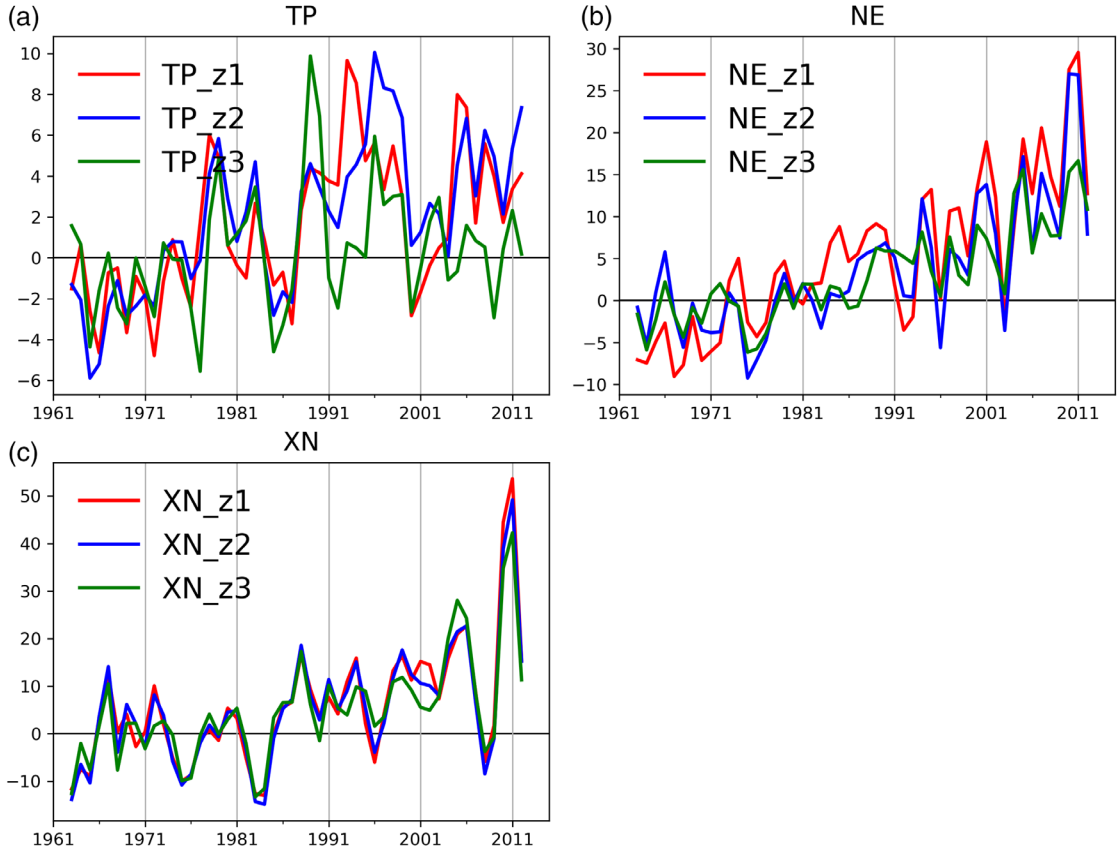

FIGURE 4 The change of winter snowfall anomaly in the Qinghai-Tibet Plateau (a), the northeast China (b), and the northern Xinjiang (c). z1, z2, and z3 indicate the Zone 1, Zone 2, and Zone 3, respectively. The temporal coverage is 1961–2015. The reference period is selected in 1961–1990. The *y*-axis is the anomaly of snowfall amount (mm). The line is smoothed by a 3-point filter [Colour figure can be viewed at wileyonlinelibrary.com]

3.3 | Change of snowfall intensity

Snowfall intensity is one of the key indicators for extreme snowfall in winter time, the fluctuations of which could affect the winter snowfall amount. It is observed from surface weather observation that snowfall intensity in the northern NE and eastern TP exhibits a remarkable upwards trend (Yulian *et al*., 2013). For snowfall intensity on grid scale, the frequency for all snowfall intensity levels (Figure 5) was higher in 1991–2015 than in 1961–1990, in both APHRO and CN05.1 snowfall data sets. In winter, light snowfall in the common months (November and December, January and March) across snow-dominant regions had a higher frequency in February. The average frequency of light snowfall in TP, NE, and XN is 3, 5, and 6 times, respectively. There was no significant change in moderate snowfall between the two periods, and the frequency of moderate snowfall on November is higher than 8 times. Heavy snowfall (Figure 5), which occurred less than once per month, was mainly concentrated in December. Snowstorms (Figure 5) mostly occurred in January. In XN, all snowfall intensity levels have been more frequent in the cold season of 1991–2015, especially for moderate and heavy snowfall (Zhao *et al*., 2011; Wang *et al*., 2013; Songzhu *et al*., 2014). In NE, the snowstorms occurred more frequently in January during 1991–2015 than during 1961–1990. This is consistent with the conclusions of a previous study, in which snowstorm frequency increased significantly at over 90.4% of the weather stations in eastern NE (Zhou *et al*., 2017). Overall, the CN05.1 snowfall data set had a greater frequency of snowfall intensity increase than APHRO. The average frequency of snowfall intensity in TP was lower than in the other two regions because of the larger area of TP. The increased snowfall frequency at different intensities is thus one reason for the snowfall increase.

Figure 5 indicates that the frequency of all snowfall intensity levels had an increasing tendency over the study period, especially light snowfall. The values in Figure 5 are the mean of regional area, which suggests that if the values are more than 1, the same snowfall intensity level occurs in all grids in that region.

Based on extreme value theory, the extreme snowfall in snow-dominant regions was smoothed using dynamically rolling 11-year windows. Figure 6 shows the extreme snowfall intensity in once-in-a-century. In the TP, the extreme snowfall

in December showed a downwards trend before 1986. Extreme snowfall in December in NE and XN showed a consistent downwards trend throughout the study period. In XN and NE, extreme snowfall reached maximum in January and was minimum in November. In general, the temporal pattern of extreme snowfall in XN and NE mainly showed a decreasing trend. However, the extreme snowfall of the TP was distinct from the other areas. The TP extreme snowfall in November, December, and January had a more complex tendency.

3.4 | Temporal change of snowfall

The first and ending date of snowy season (FDSS and EDSS, respectively), duration of the snowy season (DSS),

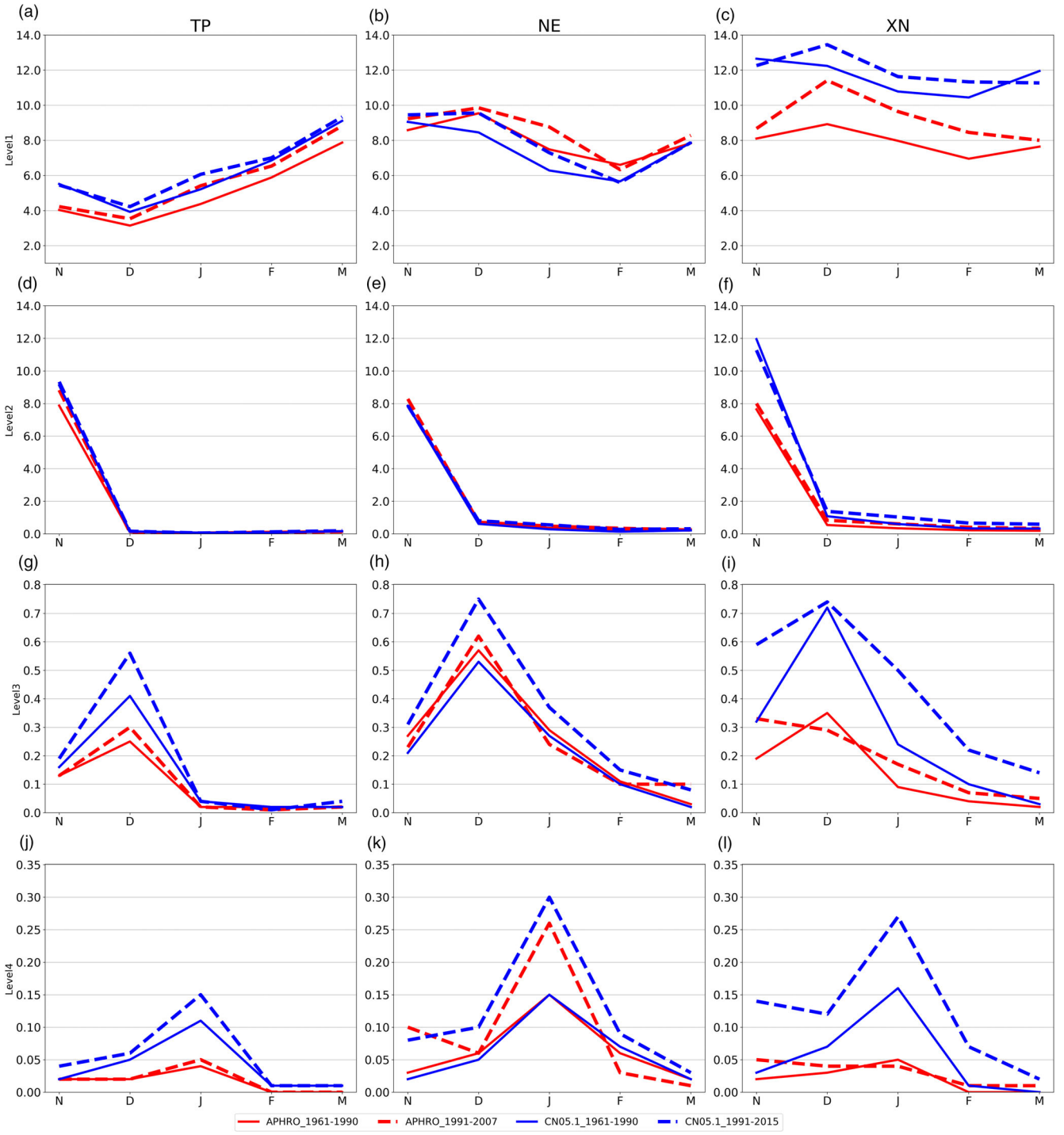

FIGURE 5 Changes of snowfall intensity frequency in snow-dominant regions. The rows are light snowfall (Level 1), moderate snowfall (Level 2), heavy snowfall (Level 3), and snowstorm (Level 4), respectively. The columns are Qinghai-Tibet Plateau (TP), northeast China (NE), and northern Xinjiang (XN). The unit is number of times [Colour figure can be viewed at wileyonlinelibrary.com]

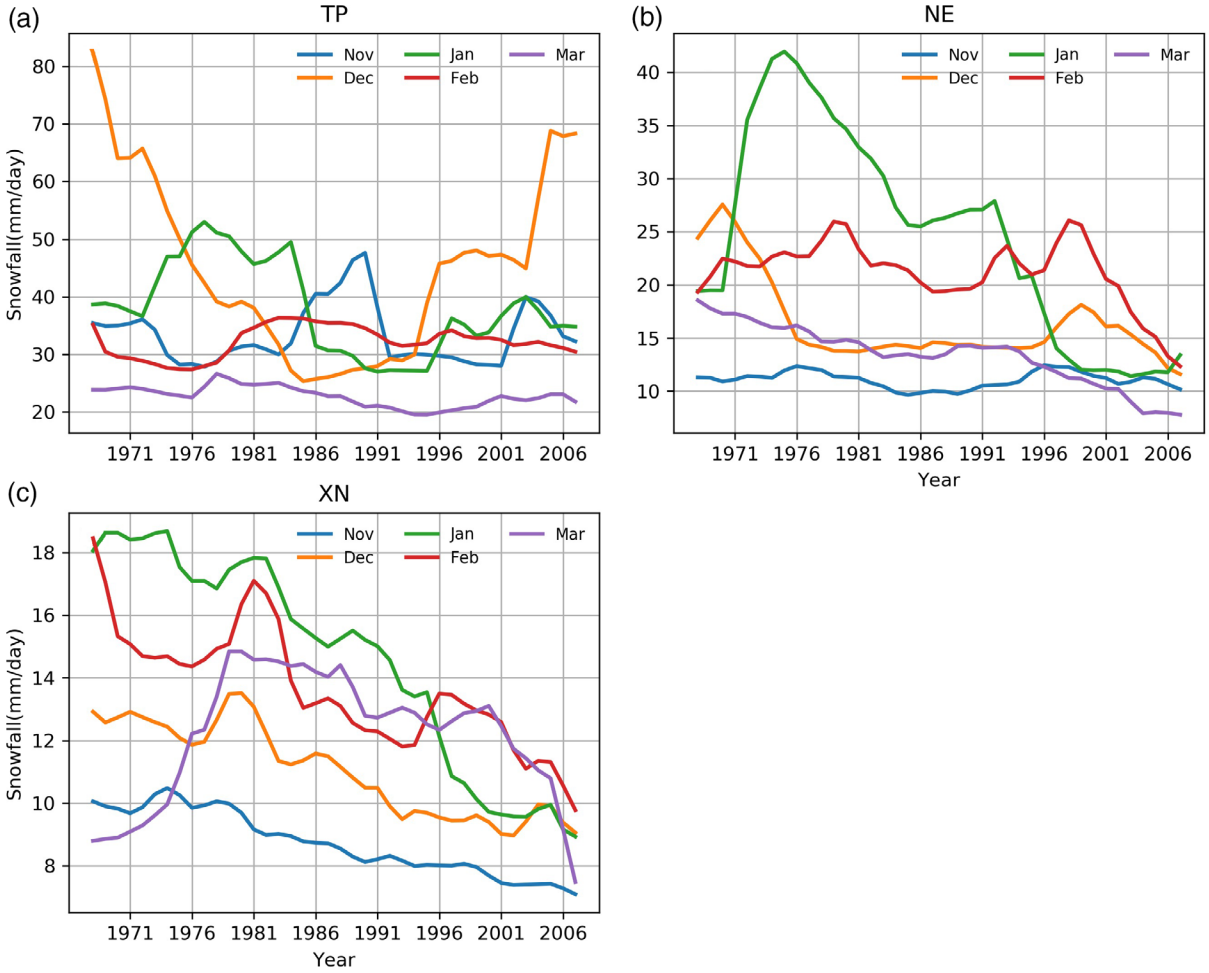

FIGURE 6 The winter extreme snowfall intensity in once-in-a-century in the Qinghai-Tibet Plateau (a), northeast China (b), and northern Xinjiang (c). The line is smoothed by a 3-point filter [Colour figure can be viewed at wileyonlinelibrary.com]

and total number of snowy days (TNSD) are statistical metrics and indicators for climatological snowfall change. In XN and TP, APHRO and CN05.1 (Figure 7a,b) both showed the FDSS in the mountainous regions was on 245th day Julian day (August). In interior and western part of TP, CN05.1 presented an earlier FDSS than APHRO. Junggar Basin (87.3°E, 45.5°N) in XN and Qaidam Basin (93.1°E, 37.5°N) in the TP have the FDSS on 330th day (Figure 7a, b). The mountainous regions in NE had the FDSS on the 270th day (September). The EDSS in NE was around 100th day (March) in both APHRO and CN05.1 (Figure 7c,d). In XN, the EDSS in the plain area was about 90th day (March) and EDSS in the Tianshan Mountains was approximately 180th day (June). Furthermore, the EDSS over most of the TP was the 180th day (June).

In Figure 7e,f, the mountainous regions in NE had a DSS of over 180 days. DSS in mountainous regions in TP and XN was typically over 270 days. Previous study with in situ observation also shows that DSS in western NE (Great Khingan Mountains) is more than 210 days and that DSS in eastern TP is even over 300 days (Yulian *et al*., 2012). The analysis with gridded data sets in this study has less DSS than one with in situ observation. The spatial pattern of TNSD in CN05.1 and APHRO was almost the same (Figure 7g,h), but CN05.1 showed more TNSD in XN and TP than in NE, especially in mountainous regions. In general, the regions with complex terrain had more snowy days.

Both APRHO and CN05.1 showed a warming signal. In 1991–2015, the FDSS was postponed by 1–4 days in all of the snow-dominant regions, compared with that in 1961–1990 (Table 3). The EDSS came early by 3–8 days compared with that in 1961–1990. The DSS was shortened by 3–8 days in the latter period. In APHRO, TNSD slightly increased between the two periods, whereas it decreased in CN05.1, except for NE. However, a decreasing trend of DSS is observed in XN (Liequn *et al*., 2013). APHRO failed to reveal this process. In general, the statistical values in CN05.1 showed a stronger warming signal than APHRO. This may be related to the APHRO's temporal coverage of 1961–2007, which is shorter than that of CN05.1.

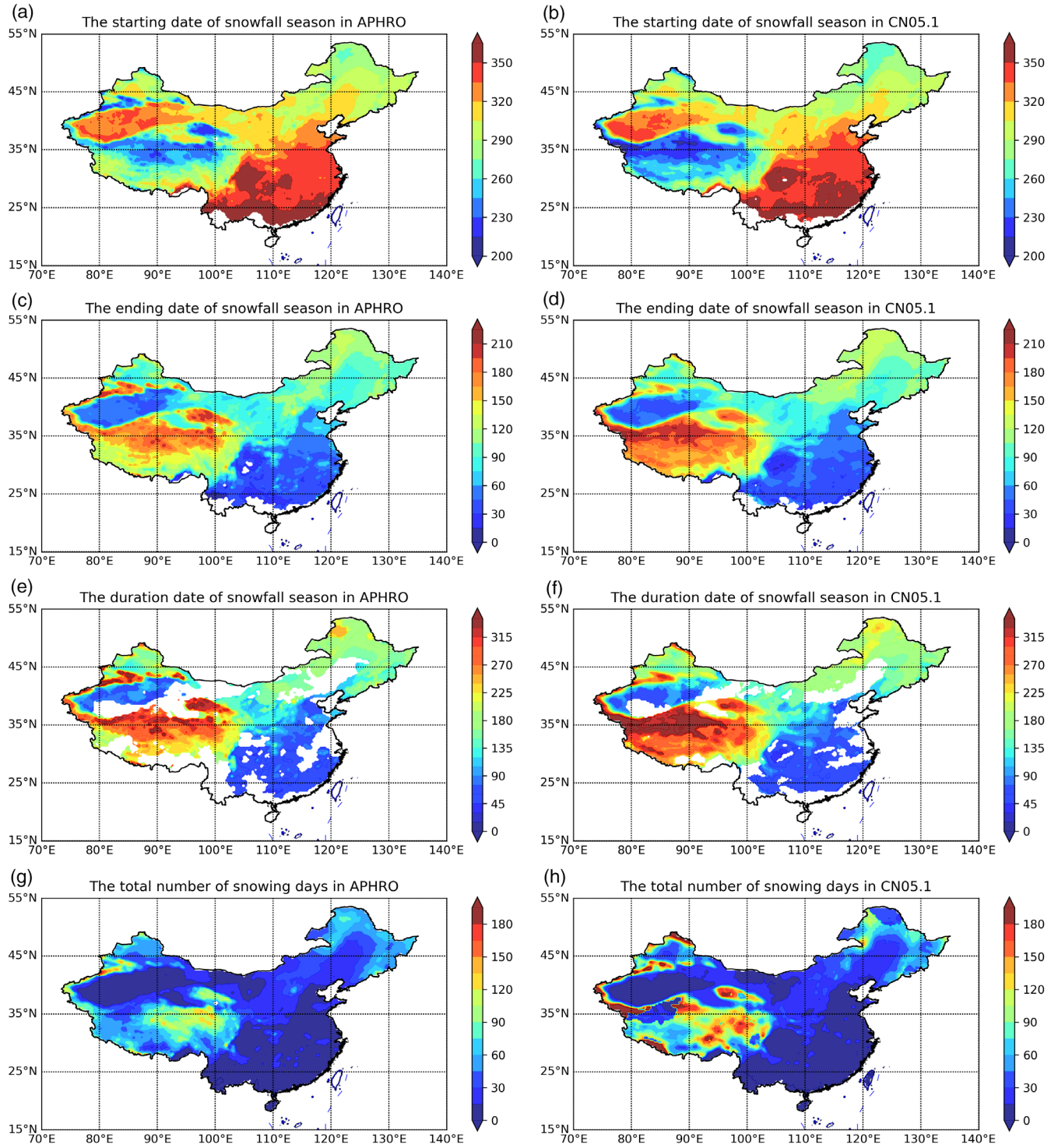

FIGURE 7 The statistical temporal information of snowfall in APHRO and CN05.1 snowfall data sets. The left column and right column is APHRO's information and CN05.1's information, respectively. The rows are the first day of snowy season, the end day of snowy season, the duration of the snowy season, and the total snowy day, respectively

3.5 | Possible reasons for snowfall change

The transportation of water vapour in the atmosphere is the source of winter snowfall, in which water vapour content and wind speed are the controlling factors for water vapour transportation. In the NCEP/NCAR reanalysis data set, air temperature at 1,000–500 hPa showed a strong warming trend (Table 4) in snow-dominant regions during 1961–2015, which indicates that the whole atmosphere is in the warming state. Snowfall in different elevation zones, however, presented the increasing trend. The thermal process could not explain snowfall change in snow-dominant regions. The geopotential height of 500 hPa

(Table 4) has increased in height in snow-dominant regions during 1961–2015. This demonstrates that the geopotential height is in an uplift state, leading to fewer weather systems (e.g., Toughs and Fronts) conductive for snowfall occurring in winter. Thus, the dynamic process could not explain snowfall change in snow-dominant regions.

Satellite observations, blended with numerical weather model simulation and satellite remote sensing data, have indicated that water vapour is increasing in Europe and the northeastern United States, which is mainly caused by the shrink of Arctic sea ice area (Liu *et al*., 2012a). The eastern China extreme snowfall in 2008 is associated with the changes of water vapour transport (Nan and Zhao, 2012). Analysis with long-term data shows that the snowfall in northeastern China is mainly affected by the local atmospheric water vapour amount before the snowfall arrivals (Sun and Wang, 2013). Therefore, the changes in atmospheric water vapour will affect the temporal and spatial patterns of snowfall. However, this is only one of the mechanisms that could explain the physical process of the changing pattern in snowfall.

The Q values on 1,000–500 hPa showed an increasing trend in XN and NE, but not on the TP. Hence, the near-surface atmospheric boundary layer has contained more water vapour over the last 55 years, which is conductive to increasing the local snowfall. Excluding the TP, the U wind and V wind at 1,000–500 hPa also showed a weakly increasing trend in snow-dominant regions. This phenomenon illustrates the strengthening intensity of near-surface water transportation. The increased water vapour from the northern Atlantic Ocean and the Arctic Ocean arrived in the snow-dominant regions with the westerlies (Yang *et al*., 2010; Liu *et al*., 2015). The change in TP was a decrease trend in Q, U wind, and V wind, which indicates less water vapour than the other regions. It was assumed that the local water cycle increased in response to the striking increase of snowfall. Nerveless, the water vapour might come from the surface evaporation in the melting of surface seasonally frozen soil, snow cover, and retreat of a glacier (Zhao *et al*., 2004; Cheng and Wu, 2007; Yao *et al*., 2012). A previous study has shown the snowfall increase in NE is mainly affected by the atmospheric water vapour content before snowy days (Sun and Wang, 2013). Therefore, it could be assumed that the increased snowfall in snow-dominant regions was mainly affected by water vapour increase. Furthermore, the wind would strengthen the water vapour transportation for snowfall. Besides, the temperature effect illustrated from Claudius's equation.

In addition to the atmospheric analysis, the frequency of snowfall occurrence by partitioning should be taken into consideration for comprehensive analysis. In this study, two approaches (surface air temperature induced method and relative humidity induced method) were employed to partition the rainfall and snowfall. The trend analysis for 1961–2015 (Table 5) showed frequencies of T_{cri} and RH_{cri} occurrence, indicating the snowy weather condition satisfied the algorithm's threshold, and showed a downwards tendency. The trend of T_{cri} frequency in TP, NE, and XN was −0.39 times/10 years, −0.46 times/10 years, and −0.76 times/10 years, respectively. The RH_{cri} frequency is −0.04 times/10 years, −0.30 times/10 years, and −0.44 times/10 years, respectively. These findings indicate that appropriate conditions for snowfall have decreased, which cannot explain the cause of the observed phenomenon of snowfall increasing. It only illustrates the snowfall intensity increase in accordance with the increased snowfall amount.

Overall, considering both the changes caused by local atmosphere and the change of snowy weather conditions, only water vapour transportation showed an increasing state and thus it could be assumed that water vapour transportation was the main cause for snowfall increase in snow-dominant regions. However, the explanation to this phenomenon remains open. In terms of Clausius's equation, the air temperature warming also could increase local water vapour content. It is therefore difficult to distinguish which is the main cause for increased snowfall in snow-dominant regions. Further studies should

TABLE 3 Statistical table of statistical snowy day data between APHRO and CN05.1 in snow-dominant regions, China

		APHRO			CN05.1		
		TP	NE	XN	TP	NE	XN
First snowy date (FDSS)	1961–1990	265.11	287.14	273.96	251.16	281.83	276.22
	1991–2015	268.76	288.39	275.21	256.99	285.28	280.86
Last snowy date (EDSS)	1961–1990	150.22	110.66	126.03	166.20	115.52	119.23
	1991–2015	144.48	105.32	125.30	158.28	111.19	116.22
Snowy season duration (DSS)	1961–1990	261.90	177.99	216.49	282.18	187.98	207.42
	1991–2015	255.58	172.70	216.81	274.39	183.44	204.52
Snowy days (TNSD)	1961–1990	62.03	56.09	64.84	93.16	60.21	92.62
	1991–2015	63.67	58.56	70.91	87.83	61.54	91.76

focus on analysing which factor is the main cause of the increasing trend of snowfall amount in snow-dominant regions.

Besides, large-scale weather systems, such as the North Atlantic Oscillation (NAO), the Arctic Oscillation (AO), and the El Niño–Southern Oscillation (ENSO), has a correlation relationship with winter snowfall in TP (Shaman and Tziperman, 2005; Xiaoge *et al*., 2010; Cuo *et al*., 2013; Wang *et al*., 2018). These climate indices indirectly indicate the atmospheric circulation change and water vapour transportation. In Figure 8, four climate indices are used to calculate the linear correlation coefficient (CC) with cold season month snowfall in CN05.1 during 1961–2015. It is found that CCs in AO (Figure 8b) and in NAO (Figure 8d) have a similar spatial pattern, with a higher CC (>0.1) in eastern TP and lower CC (<−0.1) in northern XN. This spatial pattern is distinct from others. It is found that snowstorms in 1961–2014 have a negative CC with NAO (−0.47) and AO (−0.53) in northern China (latitude >35°N), which basically agree with Figure 8b,c (Wang and Zhou, 2018). However, CC in TP is positive, especially eastern TP and further inland of TP. Therefore, when AO and NAO are at positive (negative) phase, snowfall would be more (less) in TP and less (more) in XN and NE. For MEI, CC in XN and TP, especially western TP, is relatively higher than in NE and eastern TP. This means that XN and TP would get more snowfall when MEI is at a positive phase. For AAO (Figure 8a), CC in XN and most of NE is slightly less than −0.07. In western NE, CC is more than 0.14. In some areas of western TP, CC is less than −0.14.

TABLE 4 The tendency of atmospheric variable in snow-dominant regions at 1,000–500 hPa

	TP	NE	XN
Ta (K/year)	0.273*	0.314*	0.172
HGT (m/year)	6.766*	4.465	5.309*
Q (kg kg^{-1} year^{-1})	−0.006	0.005	0.020
U wind (m s^{-1} year^{-1})	−0.089	0.059	0.055
V wind (m s^{-1} year^{-1})	−0.056	0.130	0.183*

Note. The asterisk denotes significance at p values <.01. In TP, the variables are calculated at 700–500 hPa.

TABLE 5 The tendency of thresholds for partitioning precipitation (unit: times/10 years)

	TP	NE	XN
T_{cri}	−0.39*	−0.46*	−0.76*
RH_{cri}	−0.04	−0.30*	−0.44

Note. The asterisk denotes significance at p values <.01.

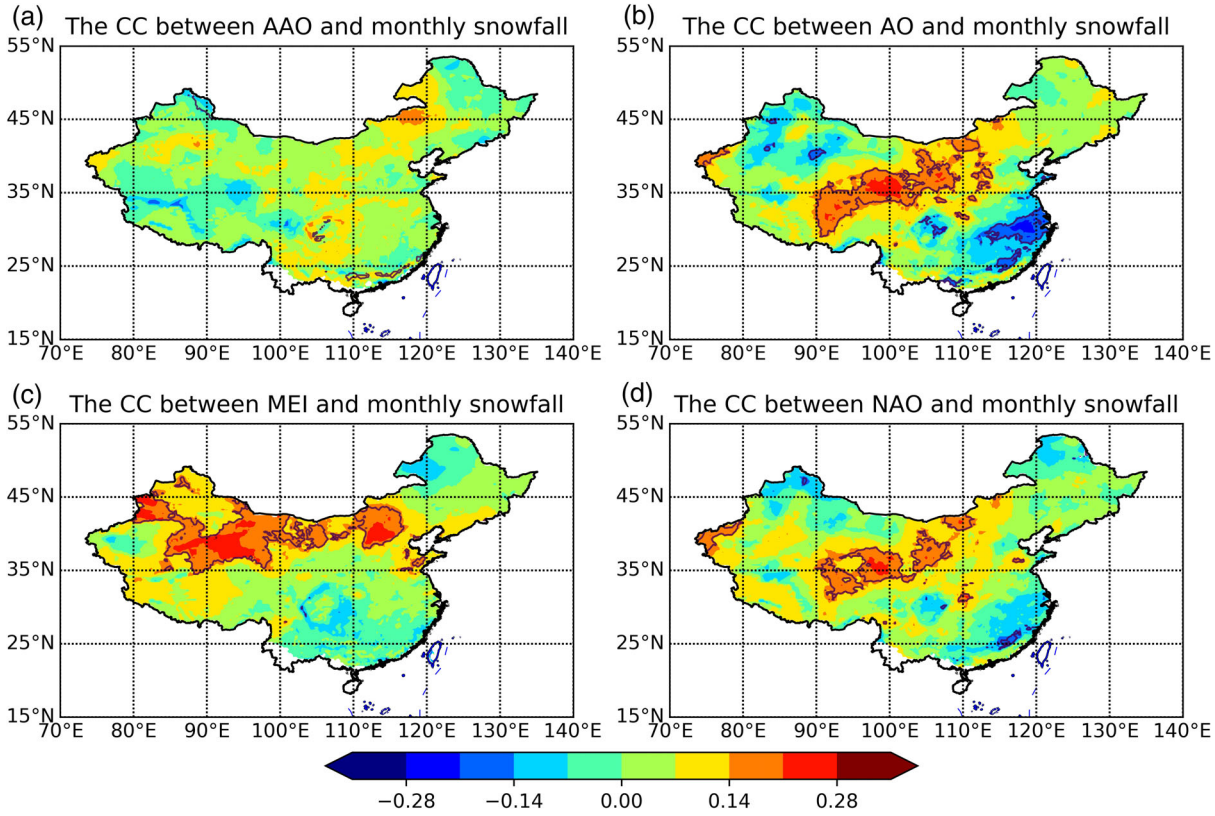

FIGURE 8 The spatial pattern of CC between monthly snowfall and climate index. The subplots (a–d) are the CC of AAO, AO, MEI, and NAO, respectively. The areas inside contour lines means that the CC is significantly (p < .01) [Colour figure can be viewed at wileyonlinelibrary.com]

TABLE 6 The linear trend of four climate indices in 1961–2015 (units: /10 years)

	AO	AAO	NAO	MEI
Cold season (Nov–Mar)	0.030 (0.388%)	0.031 (0.541%)	0.037 (0.588%)	0.009 (0.174%)
Early cold season (Nov–Dec)	0.061 (0.784%)	0.040 (0.697%)	0.084 (1.354%)	0.031 (0.589%)
Late cold season (Jan–Mar)	0.056 (0.725%)	0.069 (1.214%)	0.064 (1.034%)	0.011 (0.218%)

Note: Fraction number in parentheses is the trend over the range between climate indices' maximum and climate indices' minimum. The trend of AAO is calculated for 1979–2015.

As monthly snowfall has a relationship with four climate indices, the climate indices' trend should be analysed for 1961–2015. In Table 6, it is found that all four climate indices have an upwards trend. However, the trend of climate indices has a different relationship in different periods. For AO and NAO, the trend of climate indices in the late cold season is higher than that in the early cold season and the whole cold season, which exhibits a slight change. For MEI, the trend of climate indices in the late cold season is 0.031 (0.589%), but decreases to 0.011 (0.218%) in the early cold season. Overall, these three climate indices exhibit great changes in the early cold season than those in the late cold season. For AAO, a great reversal occurs, which has higher values of 0.069 (1.214%) in the late cold season than values of 0.031 (0.589%) in the early cold season. Thus, with the knowledge that monthly snowfall is related to climate indices, the increasing trend of climate indices indicates more snowfall in snow-dominant regions. Nevertheless, which climate indices mainly effect the increasing process of snowfall is not clear. It should be further studied.

4 | DISCUSSION

At present, the precipitation phase partition algorithm is originated from empirical experience, regardless of whether the application is satellite product, numeric weather prediction model or gridded data set extrapolated from in situ observations. However, the parameter fitted by in situ observations may not be coordinated with numeric model grids because of scale problems, especially in complex terrain with large mountains in coastal regions. For example, in the beginning of cold season, Urumqi (87°E, 40°N, elevation: 730 m) located at the foot of Tianshan Mountains, which is a transition zone between plain and alpine terrain, has a 2 m air temperature of 10°C. Assuming Urumqi is located in the centre of a 0.25° grid, the south edge will reach the Tianshan Mountains with elevation 1,500 m, for which 2 m air temperature might be 5°C or lower. When this grid is labelled with rain, if the air temperature dependent partitioning algorithm is employed, it is labelled with rainfall, for which the threshold is normally 2–3°C. However, the high land in Urumqi is more likely to receive snowfall than rainfall and thus, the grid or sub-grid cannot describe the detailed actual information. The same situation occurs in coast regions (e.g., Liaodong Peninsula [122.5°E, 40°N] and Shandong Peninsula [121°E, 37°N]). Although this study uses high resolution precipitation data (Figure 2), it still cannot solve the scale problem, which is the key limitation in this study. Furthermore, in snow-dominated regions, this scale problem usually occurs in transient season at beginning and ending of cold season. There was no significant difference among partition algorithms in other parts of the cold season. In southern China, snowfall is ordinarily considered as an extreme climate event, and the scale problem is more complicated. Thus, the scale of parameterization in precipitation phase partition will be key to improve the performance of gridded snowfall data sets in future.

In this study, the horizontal resolution of both APHRO and CN05.1 was 0.25° and thus most grids in the TP do not have sufficient in situ observation to fill the boxes. For this reason, great uncertainty exists in this region (Zhao *et al*., 2014). In Figure 2, the multiyear mean snowfall amount in CN05.1 was higher than that in APHRO, especially in the Tianshan Mountains (84°E, 43°N) and TP. First, APHRO uses no more than 800 stations for extrapolation in China against 2,400 stations in CN05.1. Second, APRHO uses the inversed distant weights algorithm to make raw gridded precipitation, whereas the plate spline algorithm is used in CN05.1. In most of NE (see Figure 7h), there was a half circle in CN05.1, which may be caused by the extrapolating algorithm. The two gridded data sets have drawbacks related to the original in situ observations and their extrapolating algorithm. Data blending and data assimilation are promising techniques with which to solve the problem in the future.

NCEP/NCAR and other long-term Reanalysis data sets have poor performance in the TP region (Wang and Zeng, 2012), which is another uncertainty factor for this study analysis. However, Chinese Reanalysis Datasets (CRA40), which include more achievement of the TP's scientific experiments, and the new generation of reanalysis data set ERA5, could enhance the performance of reanalysis data set in the TP. Recently, snow assimilation techniques have great achievement (Sun *et al*., 2004; Slater and Clark, 2006), which produce snow water equivalent data with high data quality, especially

for mountainous areas and snow covers. Some researchers have used the hydrological models (Shrestha *et al*., 2014) and the snow water equivalent-snowfall models (Broxton *et al*., 2016) to produce a simulated spatiotemporal pattern of snowfall that is closer to that of the natural environment.

5 | CONCLUSIONS

With two gridded snowfall datasets, this study analysed the snowfall spatiotemporal change, change in snowfall intensity, and the possible reasons for the change of snowfall in snow-dominant regions of China. The main conclusions are summarized below.

1. In snow-dominant regions, the mountainous regions had more snowfall than the plains regions. The snowfall data set derived from CN05.1 showed more snowfall than the APHRO snowfall data set. The difference between the data sets was possibly caused by the difference in the number of meteorological stations for each data set. Both the APHRO and CN05.1 snowfall data sets showed similar and dramatic increasing trend in most snow-dominant regions. However, a significant difference in the spatial pattern of the increasing trend was observed in the TP.
2. Comparison of the winter precipitation in indicated a significantly stronger increasing trend in the winter precipitation anomaly in China than in the NH with small uncertainties. The snowfall in winter also presents a sharply rising trend, and it was assumed that the winter snowfall contributed to the increase of the winter precipitation in China. To consider the topographic factor, the snowfall also illustrated a striking rising trend in snow-dominant regions. However, the intensity of increasing trend was not uniform in all of the altitude zones. The higher elevation zones (Zone 3) in snow-dominant regions usually had smaller rate of increase than middle elevation (Zone 2) and lower elevation zones (Zone 1).
3. In snow-dominant regions, the frequency of light snowfall significantly increased from 1961–1990 to 1991–2015, but there was little change in moderate snowfall intensity. There was also an increased frequency of heavy snowfall and snowstorms. However, the intensity of extreme snowfall intensity in once-in-a-century decreased overall in all of the snow-dominant regions. Therefore, the increase of frequency of different snowfall intensity contributes more to the increase of snowfall compared to extreme snowfall intensity in once-in-a-century.
4. Overall, the first snowy day in snow-dominant regions was postponed and the end snowy day came earlier. This has the length of the snowy season to be shortened. Considering the pattern on altitude direction, the mountainous areas had more snowy days than other snow-dominant regions.
5. The increase of winter snowfall in snow-dominant regions was mainly caused by the increase in atmospheric water content rather than the increase of frequency of weather conditions conducive to snowfall. Furthermore, monthly snowfall in XN and TP has a negative relationship with NAO and AO. Monthly snowfall in TP has a positive relationship with MEI, AO, and NAO. The values of these climate indices having an increasing trend illustrates the Westerly strengthened, which could bring more water vapour into snow-dominant regions from oceans. It may be one reason for the snowfall increasing process in snow-dominant regions.

ACKNOWLEDGEMENTS

This work was financially supported by the Key Program of the National Natural Science Foundation of China (Grant No. 91437220) and the R&D Special Fund for Public Welfare Industry (Meteorology) (Grant No. GYHY201506002), the Science & Technology Basic Resources Investigation Program of China (Grant No. 2017FY100501_5), and the National Natural Science Foundation of China (Grant No. 41501301). We acknowledge Xinjiang Key Laboratory of Water Cycle and Water Utilization in Arid Area for providing computing resources of Cluster Labrador for data processing. We thank LetPub (http://www.letpub.com/) for providing linguistic assistance during the preparation of this manuscript.

ORCID

Lei Bai https://orcid.org/0000-0002-2354-7880

REFERENCES

Barnett, T.P., Adam, J.C. and Lettenmaier, D.P. (2005) Potential impacts of a warming climate on water availability in snow-dominated regions. *Nature*, 438, 303–309. https://doi.org/10.1038/nature04141.

Borys, R.D., Lowenthal, D.H., Cohn, S.A. and Brown, W.O.J. (2003) Mountaintop and radar measurements of anthropogenic aerosol effects on snow growth and snowfall rate. *Geophysical Research Letters*, 30, 1538. https://doi.org/10.1029/2002GL016855.

Broxton, P.D., Dawson, N. and Zeng, X. (2016) Linking snowfall and snow accumulation to generate spatial maps of SWE and snow depth. *Earth and Space Science*, 3, 246–256. https://doi.org/10.1002/2016EA000174.

Chen, R.-S., Liu, J.-F. and Song, Y.-X. (2014) Precipitation type estimation and validation in China. *Journal of Mountain Science*, 11, 917–925. https://doi.org/10.1007/s11629-012-2625-x.

Chen, X., An, S., Inouye, D.W. and Schwartz, M.D. (2015) Temperature and snowfall trigger alpine vegetation green-up on the world's roof. *Global Change Biology*, 21, 3635–3646. https://doi.org/10.1111/gcb.12954.

Cheng, G. and Wu, T. (2007) Responses of permafrost to climate change and their environmental significance, Qinghai-Tibet Plateau. *Journal*

of Geophysical Research, 112, F02S03. https://doi.org/10.1029/2006JF000631.

Compo, G.P., Whitaker, J.S. and Sardeshmukh, P.D. (2006) Feasibility of a 100-year reanalysis using only surface pressure data. *Bulletin of the American Meteorological Society*, 87, 175–190. https://doi.org/10.1175/BAMS-87-2-175.

Cuo, L., Zhang, Y., Wang, Q., Zhang, L., Zhou, B., Hao, Z. and Su, F. (2013) Climate change on the northern Tibetan Plateau during 1957–2009: spatial patterns and possible mechanisms. *Journal of Climate*, 26, 85–109. https://doi.org/10.1175/JCLI-D-11-00738.1.

Dash, S.K., Parth Sarthi, P. and Panda, S.K. (2006) A study on the effect of Eurasian snow on the summer monsoon circulation and rainfall using a spectral GCM. *International Journal of Climatology*, 26, 1017–1025. https://doi.org/10.1002/joc.1299.

Davis, C.H., Li, Y., McConnell, J.R., Frey, M.M. and Hanna, E. (2005) Snowfall-driven growth in East Antarctic ice sheet mitigates recent sea-level rise. *Science*, 308, 1898–1901. https://doi.org/10.1126/science.1110662.

Deng, H., Pepin, N.C. and Chen, Y. (2017) Changes of snowfall under warming in the Tibetan Plateau. *Journal of Geophysical Research: Atmospheres*, 122, 7323–7341. https://doi.org/10.1002/2017JD026524.

Ding, B., Yang, K., Qin, J., Wang, L., Chen, Y. and He, X. (2014) The dependence of precipitation types on surface elevation and meteorological conditions and its parameterization. *Journal of Hydrology*, 513, 154–163. https://doi.org/10.1016/j.jhydrol.2014.03.038.

Duethmann, D., Peters, J., Blume, T., Vorogushyn, S. and Güntner, A. (2014) The value of satellite-derived snow cover images for calibrating a hydrological model in snow-dominated catchments in Central Asia. *Water Resources Research*, 50, 2002–2021. https://doi.org/10.1002/2013WR014382.

Fu, Q., Hou, R., Li, T., Wang, M. and Yan, J. (2018) The functions of soil water and heat transfer to the environment and associated response mechanisms under different snow cover conditions. *Geoderma*, 325, 9–17. https://doi.org/10.1016/j.geoderma.2018.03.022.

Fujiyoshi, Y., Endoh, T., Yamada, T., Tsuboki, K., Tachibana, Y. and Wakahama, G. (1990) Determination of a *Z–R* relationship for snowfall using a radar and high sensitivity snow gauges. *Journal of Applied Meteorology*, 29, 147–152. https://doi.org/10.1175/1520-0450(1990)029<0147:DOARFS>2.0.CO;2.

Harris, I., Jones, P.D., Osborn, T.J. and Lister, D.H. (2014) Updated high-resolution grids of monthly climatic observations—the CRU TS3.10 dataset. *International Journal of Climatology*, 34, 623–642. https://doi.org/10.1002/joc.3711.

Hou, A.Y., Kakar, R.K., Neeck, S., Azarbarzin, A.A., Kummerow, C. D., Kojima, M., Oki, R., Nakamura, K. and Iguchi, T. (2014) The Global Precipitation Measurement Mission. *Bulletin of the American Meteorological Society*, 95, 701–722. https://doi.org/10.1175/BAMS-D-13-00164.1.

Jiang, W., Jia, L., Xiao, T., Luobu, J. and Zhou, Z. (2016) Climate change and spatial distribution of winter snowfall over the Tibetan Plateau during 1971–2010. *Journal of Glaciology and Geogryology*, 38, 1211–1218 (in Chinese).

Jonas, T., Rixen, C., Sturm, M. and Stoeckli, V. (2008) How alpine plant growth is linked to snow cover and climate variability. *Journal of Geophysical Research*, 113, 377, G03013. https://doi.org/10.1029/2007JG000680.

Kalnay, E., Kanamitsu, M., Kistler, R., Collins, W., Deaven, D., Gandin, L., Iredell, M., Saha, S., White, G., Woollen, J., Zhu, Y., Leetmaa, A., Reynolds, R., Chelliah, M., Ebisuzaki, W., Higgins, W., Janowiak, J., Mo, K.C., Ropelewski, C., Wang, J., Jenne, R. and Joseph, D. (1996) The NCEP/NCAR 40-year reanalysis project. *Bulletin of the American Meteorological Society*, 77, 437–471. https://doi.org/10.1175/1520-0477(1996)077<0437:TNYRP>2.0.CO;2.

Ke, C.-Q., Yu, T., Yu, K., Tang, G.-D. and King, L. (2009) Snowfall trends and variability in Qinghai, China. *Theoretical and Applied Climatology*, 98, 251–258. https://doi.org/10.1007/s00704-009-0105-1.

Kobayashi, S., Ota, Y., Harada, Y., Ebita, A., Moriya, M., Onoda, H., Onogi, K., Kamahori, H., Kobayashi, C., Endo, H., Miyaoka, K. and Takahashi, K. (2015) The JRA-55 reanalysis: general specifications and basic characteristics. *Journal of the Meteorological Society of Japan*, 93, 5–48. https://doi.org/10.2151/jmsj.2015-001.

Laternser, M. and Schneebeli, M. (2003) Long-term snow climate trends of the Swiss Alps (1931–99). *International Journal of Climatology*, 23, 733–750. https://doi.org/10.1002/joc.912.

Li, S., Tang, Q., Lei, J., Xu, X., Jiang, J. and Wang, Y. (2015) An overview of non-conventional water resource utilization technologies for biological sand control in Xinjiang, northwest China. *Environmental Earth Sciences*, 73, 873–885. https://doi.org/10.1007/s12665-014-3443-y.

Li, X., Cheng, G., Jin, H., Kang, E., Che, T., Jin, R., Wu, L., Nan, Z., Wang, J. and Shen, Y. (2008) Cryospheric change in China. *Global and Planetary Change*, 62, 210–218. https://doi.org/10.1016/j.gloplacha.2008.02.001.

Li, X., Zhang, M., Wang, B., Wang, Y. and Wang, S. (2012) The change characteristics of winter snowfall, snow concentration degree and concentration period in the Tianshan Mountains. *Resources Science*, 34, 1556–1564 (in Chinese).

Liequn, H., Shuai, L. and Fengchao, L. (2013) Analysis of the variation characteristics of snow covers in Xinjiang region during recent 50 years. *Journal of Glaciology and Geogryology*, 35, 793–800 (in Chinese). https://doi.org/10.7522/j.issn.1000-0240.2013.0090.

Liu, J., Curry, J.A., Wang, H., Song, M. and Horton, R.M. (2012a) Impact of declining Arctic sea ice on winter snowfall. *Proceedings of the National Academy of Sciences of the United States of America*, 109, 4074–4079. https://doi.org/10.1073/pnas.1114910109.

Liu, X., Rao, Z., Zhang, X., Huang, W., Chen, J. and Chen, F. (2015) Variations in the oxygen isotopic composition of precipitation in the Tianshan Mountains region and their significance for the westerly circulation. *Journal of Geographical Sciences*, 25, 801–816. https://doi.org/10.1007/s11442-015-1203-x.

Liu, Y., Ren, G. and Yu, H. (2012b) Climatology of snow in China. *Scientia Geographica Sinica*, 32, 1176–1185 (in Chinese).

Liu, Y.L., Ren, G. and Yu, H.M. (2012c) Climatology of snowfall in China. *Scientia Geographica Sinica*, 32, 1176–1185 (in Chinese).

Ma, Y., Bai, L., Li, Q., Yin, G., Zhao, X. and Lanhai, L. (2016) The error analysis of the long term air temperature and precipitation in northwest China simulated by WRF model. *Journal of Glaciology and Geogryology*, 38, 77–88 (in Chinese).

Mankin, J.S., Viviroli, D., Singh, D., Hoekstra, A.Y. and Diffenbaugh, N. S. (2015) The potential for snow to supply human water demand in the present and future. *Environmental Research Letters*, 10, 114016. https://doi.org/10.1088/1748-9326/10/11/114016.

Marty, C. (2008) Regime shift of snow days in Switzerland. *Geophysical Research Letters*, 35, L12501. https://doi.org/10.1029/2008GL033998.

Matti, B., Dahlke, H.E. and Lyon, S.W. (2016) On the variability of cold region flooding. *Journal of Hydrology*, 534, 669–679. https://doi.org/10.1016/j.jhydrol.2016.01.055.

Maussion, F., Scherer, D., Mölg, T., Collier, E., Curio, J. and Finkelnburg, R. (2014) Precipitation seasonality and variability over the Tibetan Plateau as resolved by the High Asia Reanalysis. *Journal of Climate*, 27, 1910–1927. https://doi.org/10.1175/JCLI-D-13-00282.1.

Nan, S. and Zhao, P. (2012) Snowfall over central-eastern China and Asian atmospheric cold source in January. *International Journal of Climatology*, 32, 888–899. https://doi.org/10.1002/joc.2318.

National Operational Hydrologic Remote Sensing Center. (2004) *Snow Data Assimilation System (SNODAS) Data Products at NSIDC, Version 1*. Boulder, CO: National Operational Hydrologic Remote Sensing Center.

Norris, J., Carvalho, L.M.V., Jones, C. and Cannon, F. (2015) WRF simulations of two extreme snowfall events associated with contrasting extratropical cyclones over the western and central Himalaya. *Journal of Geophysical Research: Atmospheres*, 120, 3114–3138. https://doi.org/10.1002/2014JD022592.

Peiji, L. (2001) Response of Xinjiang snow cover to climate change. *Acta Meteorologica Sinica*, 59, 491–501.

Poli, P., Hersbach, H., Dee, D.P., Berrisford, P., Simmons, A.J., Vitart, F., Laloyaux, P., Tan, D.G.H., Peubey, C., Thépaut, J.-N., Trémolet, Y., Hólm, E.V., Bonavita, M., Isaksen, L. and Fisher, M. (2016) ERA-20C: an atmospheric reanalysis of the twentieth century. *Journal of Climate*, 29, 4083–4097. https://doi.org/10.1175/JCLI-D-15-0556.1.

Rauber, R.M., Olthoff, L.S., Ramamurthy, M.K. and Kunkel, K.E. (2001) Further investigation of a physically based, nondimensional parameter for discriminating between locations of freezing rain and ice pellets. *Weather and Forecasting*, 16, 185–191. https://doi.org/10.1175/1520-0434(2001)016<0185:FIOAPB>2.0.CO;2.

Rudolf, B., Hauschild, H., Rueth, W. and Schneider, U. (1994) Terrestrial precipitation analysis: operational method and required density of point measurements. In: Desbois, M. and Désalmand, F. (Eds.) *Global Precipitations and Climate Change*. Berlin-Heidelberg: Springer, pp. 173–186.

Seager, R., Kushnir, Y., Nakamura, J., Ting, M. and Naik, N. (2010) Northern Hemisphere winter snow anomalies: ENSO, NAO and the winter of 2009/10. *Geophysical Research Letters*, 37, L14703. https://doi.org/10.1029/2010GL043830.

Shaman, J. and Tziperman, E. (2005) The effect of ENSO on Tibetan Plateau snow depth: a stationary wave teleconnection mechanism and implications for the South Asian monsoons. *Journal of Climate*, 18, 2067–2079. https://doi.org/10.1175/JCLI3391.1.

Shen, Y. and Xiong, A. (2016) Validation and comparison of a new gauge-based precipitation analysis over mainland China. *International Journal of Climatology*, 36, 252–265. https://doi.org/10.1002/joc.4341.

Shrestha, M., Wang, L., Koike, T., Tsutsui, H., Xue, Y. and Hirabayashi, Y. (2014) Correcting basin-scale snowfall in a mountainous basin using a distributed snowmelt model and remote-sensing data. *Hydrology and Earth System Sciences*, 18, 747–761. https://doi.org/10.5194/hess-18-747-2014.

Slater, A.G. and Clark, M.P. (2006) Snow data assimilation via an ensemble Kalman filter. *Journal of Hydrometeorology*, 7, 478–493. https://doi.org/10.1175/JHM505.1.

Songzhu, B., Lei, H., Xiaocui, Z. and Xiuqing, X. (2014) Changing characteristics of different intensities of snowfall in Altay region, Xinjiang. *Journal of Arid Land Resources and Environment*, 28, 99–104 (in Chinese).

Sun, B. and Wang, H. (2013) Water vapor transport paths and accumulation during widespread snowfall events in northeastern China. *Journal of Climate*, 26, 4550–4566. https://doi.org/10.1175/JCLI-D-12-00300.1.

Sun, C., Walker, J.P. and Houser, P.R. (2004) A methodology for snow data assimilation in a land surface model. *Journal of Geophysical Research*, 109, D08108. https://doi.org/10.1029/2003JD003765.

Sun, J., Wang, H., Yuan, W. and Chen, H. (2010a) Spatial-temporal features of intense snowfall events in China and their possible change. *Journal of Geophysical Research*, 115, 373. https://doi.org/10.1029/2009JD013541.

Sun, X., Luo, Y., Zhang, X. and Gao, Y. (2012) Analysis on snowfall change characteristic of China in recent 46 years. *Plateau Meteorology*, 29, 1594–1601 (in Chinese).

Sun, X., Sun, Z. and Luo, Y. (2010b) Characteristics of snowfall from 1960 to 2005 in northeast China. *Journal of Meteorology and Environment*, 26, 1–5 (in Chinese).

Thériault, J.M., Stewart, R.E., Milbrandt, J.A. and Yau, M.K. (2006) On the simulation of winter precipitation types. *Journal of Geophysical Research*, 111, D18202. https://doi.org/10.1029/2005JD006665.

Tong, K., Su, F., Yang, D., Zhang, L. and Hao, Z. (2014) Tibetan Plateau precipitation as depicted by gauge observations, reanalyses and satellite retrievals. *International Journal of Climatology*, 34, 265–285. https://doi.org/10.1002/joc.3682.

Uppala, S.M., KÅllberg, P.W., Simmons, A.J., Andrae, U., Bechtold, V. D.C., Fiorino, M., Gibson, J.K., Haseler, J., Hernandez, A., Kelly, G.A., Li, X., Onogi, K., Saarinen, S., Sokka, N., Allan, R.P., Andersson, E., Arpe, K., Balmaseda, M.A., Beljaars, A.C.M., van de Berg, L., Bidlot, J., Bormann, N., Caires, S., Chevallier, F., Dethof, A., Dragosavac, M., Fisher, M., Fuentes, M., Hagemann, S., Hólm, E., Hoskins, B.J., Isaksen, L., Janssen, P.A.E.M., Jenne, R., Mcnally, A.P., Mahfouf, J.-F., Morcrette, J.-J., Rayner, N.A., Saunders, R.W., Simon, P., Sterl, A., Trenberth, K.E., Untch, A., Vasiljevic, D., Viterbo, P. and Woollen, J. (2005) The ERA-40 re-analysis. *Quarterly Journal of the Royal Meteorological Society*, 131, 2961–3012. https://doi.org/10.1256/qj.04.176.

Wang, A. and Zeng, X. (2012) Evaluation of multi-reanalysis products with in situ observations over the Tibetan Plateau. *Journal of Geophysical Research*, 117, 5102. https://doi.org/10.1029/2011JD016553.

Wang, J., Zhang, M., Wang, S., Ren, Z., Che, Y. and Qiang, F. (2017) Change of snowfall/rainfall ratio in Xinjiang during the period of 1961–2013. *Arid Zonde Research*, 34, 889–897 (in Chinese). https://doi.org/10.13866/j.azr.2017.04.23.

Wang, J., Zhang, M., Wang, S., Ren, Z., Che, Y., Qiang, F. and Qu, D. (2016a) Decrease in snowfall/rainfall ratio in the Tibetan Plateau from 1961 to 2013. *Journal of Geographical Sciences*, 26, 1277–1288. https://doi.org/10.1007/s11442-016-1326-8.

Wang, J., Zhang, M., Wang, S., Ren, Z., Che, Y. and Zhang, F. (2016b) Change of snowfall/rainfall ratio in the Tibetan Plateau based on a gridded dataset with high resolution during 1961–2013. *Acta Geographica Sinica*, 71, 142–152 (in Chinese). https://doi.org/10.11821/dlxb201601011.

Wang, S.P., Jiang, F.Q., Hu, R.J. and Zhang, Y.W. (2013) Temporal and spatial variability of extreme snowfall indices over northern Xinjiang from 1959/1960 to 2008/2009. *Natural Hazards and Earth System Sciences Discussion*, 1, 7059–7092. https://doi.org/10.5194/nhessd-1-7059-2013.

Wang, X. (2008) *Research of Snow Characteristics in Qilian Mountains Based on Satellite RS*. Beijing: Chinese Academy of Meteorological Sciences (in Chinese).

Wang, X., Pang, G. and Yang, M. (2018) Precipitation over the Tibetan Plateau during recent decades: a review based on observations and

simulations. *International Journal of Climatology*, 38, 1116–1131. https://doi.org/10.1002/joc.5246.

Wang, Z.Y. and Zhou, B.T. (2018) Large-scale atmospheric circulations and water vapor transport influencing interannual variations of intense snowfalls in northern China. *Chinese Journal of Geophysics*, 61, 2654–2666 (in Chinese). https://doi.org/10.6038/cjg2018L0405.

Willmott, C.J. and Matsuura, K. (2001) Terrestrial air temperature and precipitation: Monthly and annual time series (1950–1999). Available at: http://climate.geog.udel.edu/~climate/html_pages/README.ghcn_ts2.html.

Wu, J. and Gao, X. (2013) A gridded daily observation dataset over China region and comparison with the other datasets. *Chinese Journal of Geophysics*, 56, 1102–1111 (in Chinese). https://doi.org/10.6038/cjg20130406.

Xiaoge, X., Zhou, T. and Yu, R. (2010) Increased Tibetan Plateau snow depth: an indicator of the connection between enhanced winter NAO and late-spring tropospheric cooling over East Asia. *Advances in Atmospheric Sciences*, 27, 788–794. https://doi.org/10.1007/s00376-009-9071-x.

Xu, X. (2011) Spatiotemporal variation and regional distribution characteristics of snowfall in China from 1970 to 2000. *Journal of Glaciology and Geogryology*, 33, 497–503 (in Chinese).

Yamaguchi, S., Abe, O., Nakai, S. and Sato, A. (2011) Recent fluctuations of meteorological and snow conditions in Japanese mountains. *Annals of Glaciology*, 52, 209–215. https://doi.org/10.3189/172756411797252266.

Yang, L., Shi, Y. and Tang, H. (2010) Causes of winter precipitation anomalies in northern Xinjiang. *Journal of Applied Meteorological Science*, 21(4), 491–499 (in Chinese). https://doi.org/10.3969/j.issn.1001-7313.2010.04.013.

Yang, Z.-L., Dickinson, R.E., Robock, A. and Vinnikov, K.Y. (1997) Validation of the snow submodel of the biosphere–atmosphere transfer scheme with Russian snow cover and meteorological observational data. *Journal of Climate*, 10, 353–373. https://doi.org/10.1175/1520-0442(1997)010<0353:VOTSSO>2.0.CO;2.

Yao, T., Thompson, L., Yang, W., Yu, W., Gao, Y., Guo, X., Yang, X., Duan, K., Zhao, H., Xu, B., Pu, J., Lu, A., Xiang, Y., Kattel, D.B. and Joswiak, D. (2012) Different glacier status with atmospheric circulations in Tibetan Plateau and surroundings. *Nature Climate Change*, 2, 663–667. https://doi.org/10.1038/nclimate1580.

Yasutomi, N.A., Hamada, A. and Yatagai, A. (2011) Development of a long-term daily gridded temperature dataset and its application to rain/snow discrimination of daily precipitation. *Global Environmental Research*, 15, 165–172.

Yatagai, A., Kamiguchi, K., Arakawa, O., Hamada, A., Yasutomi, N. and Kitoh, A. (2012) APHRODITE: constructing a long-term daily gridded precipitation dataset for Asia based on a dense network of rain gauges. *Bulletin of the American Meteorological Society*, 93, 1401–1415. https://doi.org/10.1175/BAMS-D-11-00122.1.

Yulian, L., Guoyu, R. and Hongmin, Y. (2012) Climatology of snow in China. *Scientia Geographica Sinica*, 32, 1176–1185 (in Chinese). https://doi.org/10.13249/j.cnki.sgs.2012.10.014.

Yulian, L., Guoyu, R., Hongmin, Y. and Hengyuan, K. (2013) Climatic characteristics of intense snowfall in China with its variation. *Journal of Applied Meteorological Science*, 24, 304–313 (in Chinese).

Zhang, D., Cong, Z. and Ni, G. (2016a) Snowfall changes in China during 1956–2010. *Journal of Tsinghua University (Science & Technology)*, 56, 381–393 (in Chinese).

Zhang, F., Bai, L., Li, L. and Wang, Q. (2016b) Sensitivity of runoff to climatic variability in the northern and southern slopes of the Middle Tianshan Mountains, China. *Journal of Arid Land*, 8, 681–693. https://doi.org/10.1007/s40333-016-0015-x.

Zhang, F.-Y., Li, L.-H., Ahmad, S. and Li, X.-M. (2014) Using path analysis to identify the influence of climatic factors on spring peak flow dominated by snowmelt in an alpine watershed. *Journal of Mountain Science*, 11, 990–1000. https://doi.org/10.1007/s11629-013-2789-z.

Zhao, C., Wang, J., Yan, X., Wang, Y. and Luo, Y. (2009) Climatic Characteristics and Regionalization of Winter snowfall in northeast China. *Journal of Natural Disasters*, 18, 29–35 (in Chinese). https://doi.org/10.13577/j.jnd.2009.0505.

Zhao, L., Ping, C.-L., Yang, D., Cheng, G., Ding, Y. and Liu, S. (2004) Changes of climate and seasonally frozen ground over the past 30 years in Qinghai-Xizang (Tibetan) Plateau, China. *Global and Planetary Change*, 43, 19–31. https://doi.org/10.1016/j.gloplacha.2004.02.003.

Zhao, Y., Cui, C. and Li, X. (2011) Climatic characteristics of winter precipitation in Northern Xinjiang Region. *Journal of Glaciology and Geogryology*, 33, 292–299 (in Chinese). https://doi.org/10.13448/j.cnki.jalre.2014.08.009.

Zhao, Y., Zhu, J. and Xu, Y. (2014) Establishment and assessment of the grid precipitation datasets in China for recent 50 years. *Journal of the Meteorological Sciences*, 34, 414–420 (in Chinese).

Zhou, X., Zhao, C., Cui, Y., Zhan, X., Liu, M., Ao, X., Yi, X., Lin, R. and Zhang, H. (2017) Variation characteristics of different levels of snow in Liaoning Province. *Journal of Glaciology and Geogryology*, 4, 720–732 (in Chinese). https://doi.org/10.7522/j.issn.1000-0240.2017.0082.

Zhu, X., Zhang, M., Wang, S., Li, X., Dong, L. and Ren, Z. (2014) Spatiotemporal variation patterns of the beginning and ending dates of snowfall, and snowfall days. *Chinese Journal of Ecology*, 33, 761–770 (in Chinese).

How to cite this article: Bai L, Shi C, Shi Q, *et al.* Change in the spatiotemporal pattern of snowfall during the cold season under climate change in a snow-dominated region of China. *Int J Climatol*. 2019;39:5702–5719. https://doi.org/10.1002/joc.6182